ChemPubSoc Europe
DOI: 10.1002/cphc.201501036
CHEMPHYSCHEM Articles

VIP *Very Important Paper*

Oxygen Reduction on Ag(100) in Alkaline Solutions—A Theoretical Study

Aleksej Goduljan,[a] Leandro Moreira de Campos Pinto,[a] Fernanda Juarez,[a] Elizabeth Santos,[a, b] and Wolfgang Schmickler*[a]

Silver is much more reactive to oxygen than gold; nevertheless, in alkaline solutions, the rates of oxygen reduction on both metals are similar. To explain this phenomenon, the first, rate-determining step of oxygen reduction on Ag(100) is determined by a combination of DFT, molecular dynamics, and electrocatalysis theory. In vacuum, oxygen is adsorbed on Ag(100), but in the electrochemical environment, the adsorption energy is offset by the loss of hydration energy as the molecule approaches the surface. As a result, the first electron transfer should take place in an outer-sphere mode. Previously, the same mechanism for oxygen reduction on Au(100) has been predicted, and these calculations have been repeated by using a more advanced version of the electrocatalysis theory discussed herein to confirm previous conclusions. The theoretical results compare well with experimental data.

1. Introduction

Generally speaking, oxygen reduction is faster in alkaline than in acid solutions; it does not require expensive transition metals as catalysts, but proceeds with a reasonable rate on cheaper materials, such as the coinage metals silver and gold. For a recent review of oxygen reduction in alkaline solutions, see Ref. [1], which also contains references to older works. Usually, the first electron-transfer step occurs according to Reaction (R1):

$$O_2 + e^- \rightarrow O_2^- \qquad (R1)$$

and determines the overall rate.[2] It has been suggested that this step takes place in outer-sphere mode.[3] In this case, the standard equilibrium potential is about −0.3 V SHE, compared with a value of 0.4 V SHE for the overall reaction at pH 14. However, when this first step is slow and subsequent steps are fast, the concentration of O_2^- is low, and for concentrations of the order of 10^{-6}–10^{-7} M the overpotential is reduced to about 0.3 V, which is compatible with the onset potential observed on gold and silver.[4–6] Notably, this argument excludes reactions between two O_2^- ions because the concentration is too low.

In a recent study,[7] we investigated Reaction (R1) on Au(100) and concluded that indeed it took place in an outer-sphere mode without adsorption, and with an energy of activation only a little lower than the value predicted by Marcus theory. However, Au(100) is special because the energy of adsorption of O_2 from the vacuum is close to zero.[8] In contrast, Ag(100) is a good oxidation catalyst in ultrahigh vacuum,[9] and is quite reactive to O_2, with an adsorption energy of −0.4 eV.[10] In addition, there is substantial charge transfer from silver to the adsorbed particle, resulting in a superoxo-like adsorbate.[11] This raises the question if, in contrast to Au(100), Reaction (R1) takes place in an inner-sphere mode on Ag(100), upon which the product is adsorbed. On the other hand, the experimental results for oxygen reduction on Au(100) and Ag(100) are similar, which suggests that the mechanism is the same.

To resolve this question, we have investigated the first step of oxygen reduction on Ag(100) by applying a theory developed in our own group, which we have previously applied to Au(100). At the same time, we have improved our calculations by including results from molecular dynamics for the reacting particles. Therefore, we have recalculated the free energy surface for Reaction (R1) on Au(100), so that the results for the two metals are comparable.

2. Results and Discussion

To focus on chemical physics and not on formalism, the theoretical method is given in the Computational Details section. Instead, we begin with the results of our calculations.

2.1. Adsorption from the Vacuum

In agreement with other researchers,[11] we found that the O_2 molecule adsorbed at a distance of about 2.1 Å. As shown in Figure 1, it sits over a fourfold hollow site, with its axis parallel to the surface and bridging two silver atoms. During reduction, the oxygen molecule approaches the surface; therefore, we have calculated the energy and charge on the molecule as a function of the distance, by keeping its orientation and posi-

[a] A. Goduljan, Dr. L. M. de Campos Pinto, Dr. F. Juarez, Dr. E. Santos, Prof. Dr. W. Schmickler
Institute of Theoretical Chemistry, Ulm University
89069 Ulm (Germany)
[b] Dr. E. Santos
Facultad de Matemática, Astronoma y Fsica, IFEG-CONICET
Universidad Nacional de Córdoba, Córdoba (Argentina)

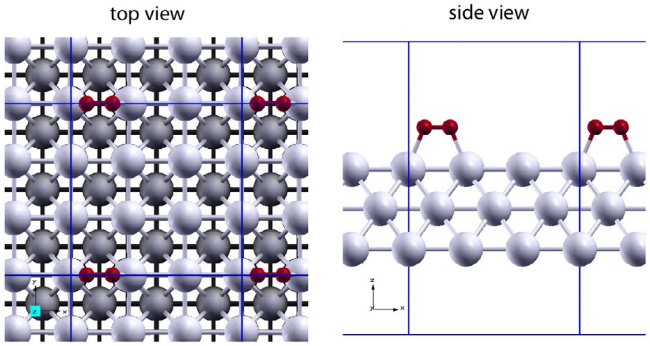

Figure 1. Configuration of O_2 adsorbed on Ag(100).

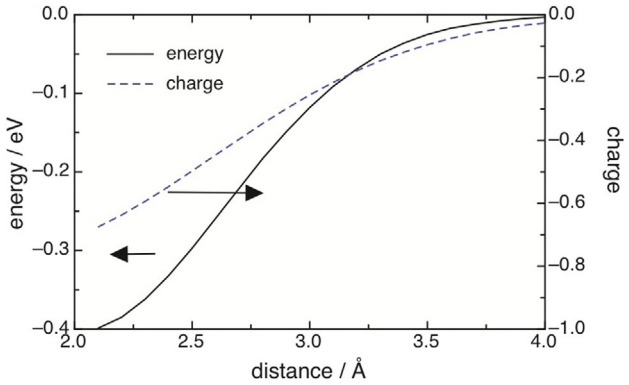

Figure 2. Energy and charge on the O_2 molecule as a function of distance.

tion parallel to the surface fixed. The charge was calculated by integrating over the electronic densities of states up to the Fermi level. As shown on Figure 2, the energy decreases continuously and, at the same time, the molecule acquires a negative charge. We obtained an adsorption energy of about −0.4 eV, which was a little higher (less favorable) than the value given in Ref. [11], but in agreement with the experimental value.[10] The adsorbed molecule has a negative charge of about −0.7, and thus, has a distinct ionic character. Beyond a separation of 4.1 Å, the energy shows a discontinuity, which is caused by the well-known difficulty of applying DFT to accurately describe the isolated O_2 molecule.[12] We only require the energy at short distances, at which this problem does not arise.

Only the p_z orbital, which is directed perpendicularly to the surface, interacts noticeably with the silver surface. Figure 3 shows its density of states (DOS) both at a large separation and in the adsorbed state. Naturally, the DOS shows spin polarization. The interaction between the two oxygen atoms splits each spin orbital into a bonding, $1\pi_u$, and an antibonding, $1\pi_g$, molecular orbital. In our convention, both the bonding and antibonding parts of the down spin orientation are filled. For the other orientation, the bonding part is filled and at large distances the antibonding part is empty. As the molecule approaches the surface, the antibonding part becomes partially filled (Figure 3, right). In the adsorbed state, at low energies, both π spin orbitals are split by the interaction with the sp band of Ag(100). At large distances, both π_g orbitals have the same DOS; however, the DOS of the π_g orbital formed from the p_y orbitals remain practically unchanged as the molecule approaches the surface.

In the course of Reaction (R1), the antibonding $1\pi_g$ formed by the p_z spin up orbitals is filled. We therefore focus on the interaction of this spin orbital with the silver surface. According to our theory (see the Computational Details section), we need the interaction constants with the d and sp bands as a function of the distance—more precisely, we need the squares of these constants. These values are shown in Figure 4; the interaction with the sp band is long range, whereas only the adsorbed state interacts with the d band.

2.2. Potentials of Mean Force

Solvation plays a crucial role in electrochemical reactions, and is equally important in our theory. The energies of solvation of the reactants depend on their separation from the electrode surface. The change in solvation energy with distance is given by the potential of mean force (pmf), which we have investi-

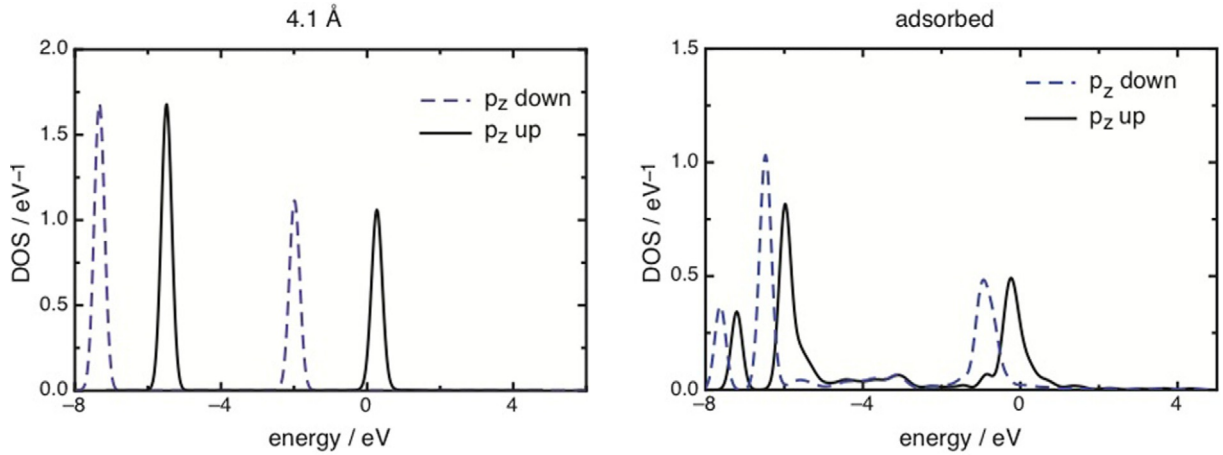

Figure 3. DOS of the p_z orbitals at a large distance (left) and in the adsorbed state (right). The Fermi level has been taken as zero energy.

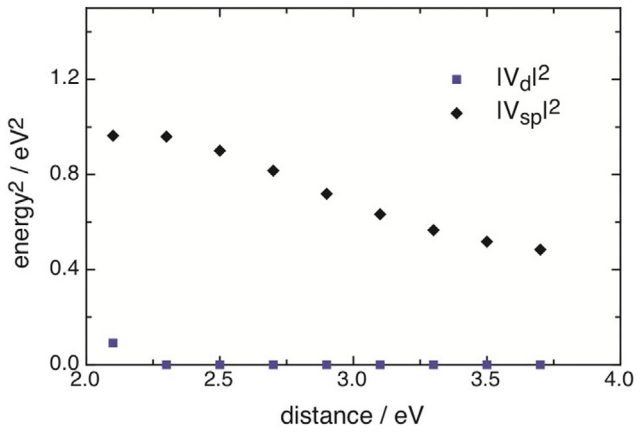

Figure 4. Squares of the coupling constants of the spin-up antibonding orbital with the d and sp bands of Ag(100).

gated by molecular dynamics (details are given in the Computational Details section).

We performed these calculations for the approach to both the Ag(100) and Au(100) surfaces, and obtained identical results. The pmf of both the molecule and anion increase towards the surface, as their hydration becomes weaker (Figure 5). This effect is stronger for the molecule, for which

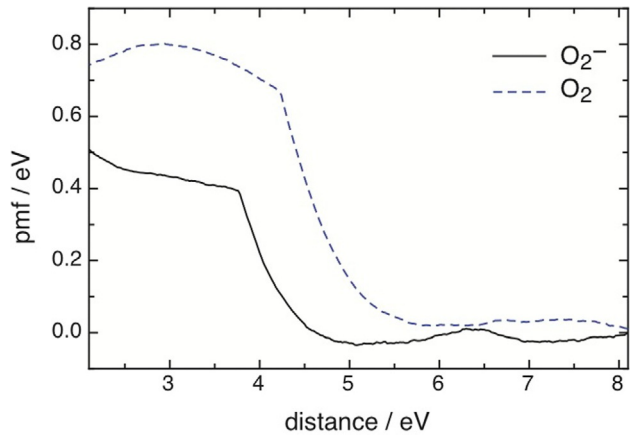

Figure 5. Potentials of mean force for the approach of O_2^- and O_2 to the electrode surface. These curves are the same for Ag(100) and Au(100).

the pmf begins to rise at about 6 Å, than that for the anion, for which it even has a slight minimum near 5 Å before it starts to rise. Considering that the hydration energy of the anion is about −3.9 eV, the increase in energy towards the surface is moderate. In contrast, for the molecule, the increase in the pmf is higher than that of the absolute value of solvation energy in the bulk. We attribute this to an exclusion effect: water likes to form a hydrogen-bonded network on the surface and expels the molecule, the solvation shell of which is much weaker than that of the anion.

In previous studies on metal deposition, we considered the approach of small metal ions towards an electrode surface and concluded that they could get very close to the surface without loss of solvation energy.[13] This is not true for the larger superoxide ion and oxygen molecule. We show below that this has important consequences for oxygen reduction.

2.3. First Step in Oxygen Reduction

We now have the ingredients we need to calculate the free energy surface for Reaction (R1). As pointed out previously,[14] with our theory, we can plot such surfaces for various electrode potentials. In Figure 6, we present the surface for the po-

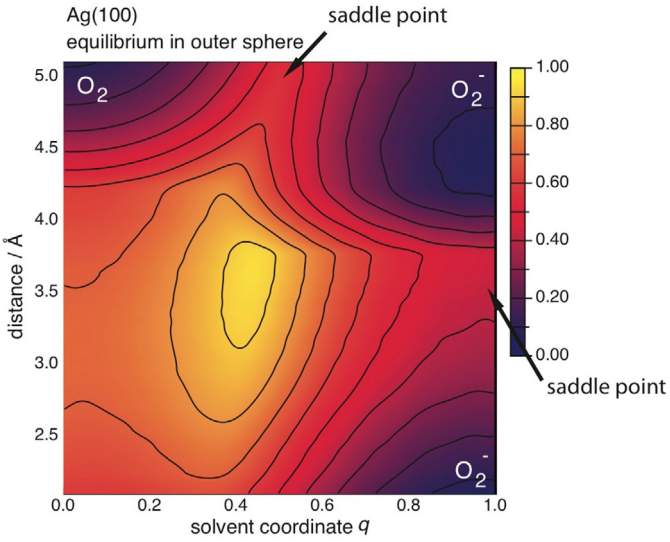

Figure 6. Free energy surface Reaction (R1) on Ag(100). The electrode potential is for equilibrium in the outer-sphere mode.

tential if the reaction is in equilibrium in the outer sphere. As usual, we have plotted the free energy as a function of the distance, d, of the reactant from the surface and of the solvent coordinate.[15] A quick reminder: the solvent coordinate characterizes the state of the solvent; it takes on the value q, if the solvent were in equilibrium with a reactant of charge $-q$. At $d=5$ Å and $q=0$, we see a minimum that corresponds to the uncharged O_2 molecule; towards the bulk of the solution this extends into a valley. We have chosen the energy zero such that the energy is zero at this minimum. Likewise, at large distances, but at $q=1$, the minimum for the anion is found; again this extends into a valley towards the bulk, but it has a real shallow minimum that corresponds to the slight minimum in the pmf observed in Figure 5. These two minima are separated by a saddle point with an energy of 0.5 eV. A transition between these minima corresponds to outer-sphere electron transfer, so according to Marcus theory,[16] the activation energy should correspond to $\lambda/4$, in which λ is the energy of reorganisation. As we have argued previously,[14,19] in aqueous solutions, λ is half the absolute value of the energy of hydration (−3.9 eV in the bulk), so this activation energy agrees with Marcus theory. Notably, close to the surface, λ decreases a little as the absolute value of energy of solvation becomes smaller, in accordance with the pmf for the anion.

Right on the electrode surface, at $q=1$, there is a third minimum that corresponds to the adsorbed state. Due to the effect of solvation, which favors charged particles, its charge is -1, which is somewhat lower than that for the adsorbed state in a vacuum (see Figure 2). Its energy is practically the same as that of the other two minima. This is the result of a compensation effect: the interaction with the metal lowers the energy by 0.4 eV (see Figure 2), but the pmf is higher than that in the bulk by about 0.5 eV (see Figure 5). A little extra energy is gained by the change in the charge. The saddle point that separates the ionic state in the bulk from the one at the surface has an activation energy of about 0.4 eV. Within the accuracy of our calculations, this is of the same order of magnitude as the saddle point for the outer-sphere step.

We have also performed calculations for a cathodic overpotential of $\eta=0.2$ V, which makes reduction more favorable. The effect on the outer-sphere pathway is straightforward: The energy of the ion is lowered by $-e_0\eta$, whereas that of the molecule is unchanged, and the saddle point is lowered by the order of 0.1 V to give a transfer coefficient of $\alpha\approx0.5$. The effect on the rest of the surface requires a model for the variation of potential near the surface. We have chosen a simple model, in which the effect of the overpotential decays linearly between $d=5.1$ Å, and the electrode surface, at which its effect vanishes. However, the qualitative conclusions are independent of the details of this decay. The corresponding surface is shown in Figure 7. Because the effect of the overpotential vanishes right on the surface, the energy of the adsorbed state is unchanged, and is now higher than that of the anion in the solution.

Blizanac et al. performed a thorough investigation of oxygen reduction on single-crystal silver in alkaline solutions.[4] They observed onset potentials of the order of 0.9 V versus RHE, which was compatible with an outer-sphere mechanism, as discussed in the Introduction. The onset potential should be close to the potential at which outer-sphere transfer is in equilibrium. From the temperature dependence of the currents, they determined the activation energies. For an electrode potential of 0.8 V versus RHE, which translated into an overpotential of about 0.1 V for the outer-sphere reaction, they observed activation energies of the order of 0.3 eV, which were compatible with our theoretical values. The measured transfer coefficients are close to 0.5, in agreement with our results and typical for an outer-sphere mechanism.

Thus, our results suggest the following pathway: at equilibrium, the first step in oxygen reduction takes place in the outer-sphere mode. The energy of the adsorbed species is about the same as that of the anion in solution, so the two species can interchange. The direct pathway from O_2 to the adsorbed anion is not favorable because of the strong increase of the pmf of the molecule near the surface (see Figure 5). Application of a cathodic overpotential favors the anion in solution, so that the adsorbed state becomes less favorable.

2.4. Au(100) Revisited

Recently, we investigated the same reaction on a Au(100) surface,[7] on which the adsorption energy of the O_2 molecule was practically zero.[8,17,18] We used the same method as that described herein, but because the pmfs for the molecule and anion were not available at that time, we used a simpler model for the solvation effects. To obtain comparable results for Au(100) and Ag(100), we have recalculated the free energy surface for Au(100); the result is shown in Figure 8. There are only two minima: one for the molecule and one for the anion, and both are far from the electrode surface. In particular, there is no stable adsorbed state. In comparison with the results reported in Ref. [7], the minimum for the anion has shifted to a somewhat larger distance; this is caused by the increase of

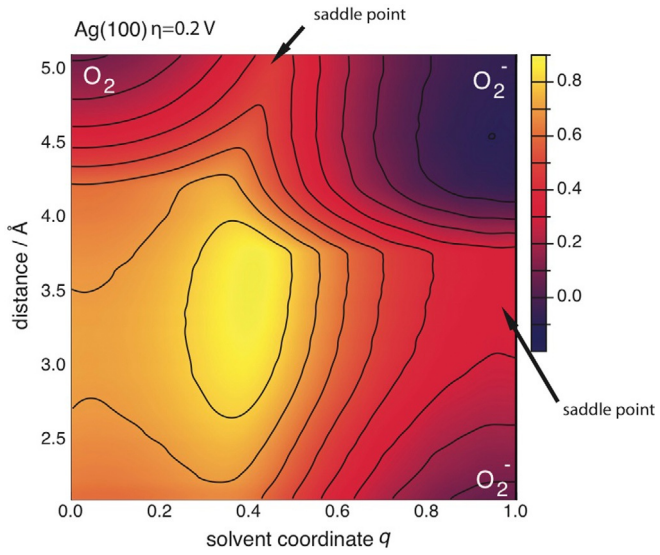

Figure 7. Free energy surface for Reaction (R1) on Ag(100) for a cathodic overpotential of $\eta=0.2$ V.

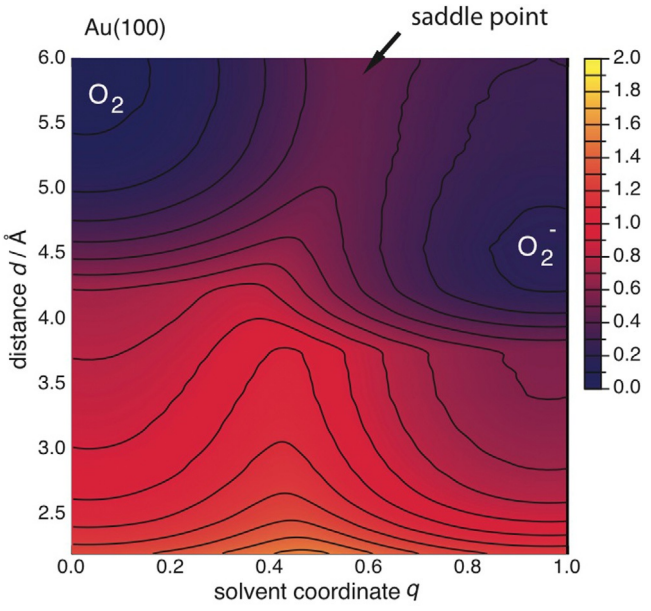

Figure 8. Free energy surface for Reaction (R1) on Au(100). The electrode potential is for equilibrium in the outer-sphere mode.

the pmf for the anion in this region. Nevertheless, the conclusions are the same as before: neither the reactant nor the product are adsorbed, and the reaction takes place in an outer-sphere mode, with an activation energy of about $\lambda/4$ at equilibrium.

3. Conclusions

Even though silver is much more reactive than gold, the first electron transfer step also takes place in an outer sphere mode. The principal reason is that the negative energy of adsorption of the O_2 molecule is offset by the energy required to take the reactant to the surface, in other words by the loss of solvation. Thus, our results highlight the importance of solvation effects on electrochemical reactions.

At the equilibrium potential for the outer sphere mode, the energies for the molecule in solution, the anion in solution, and the adsorbed anion are about the same. The energies of activation between these states are of the order of 0.4–0.5 eV. The application of a cathodic overpotential makes the anion in the solution the most favorable state.

For simple electron transfer reactions, such as $[Ru(NH_3)_6]^{2+} \rightleftharpoons [Ru(NH_3)_6]^{3+} + e^-$, which take place in the outer sphere, the rate is independent of the electrode material.[20–22] Theefore, why is the rate of oxygen reduction in alkaline solutions not exactly the same on all materials for which the first step is outer sphere? Reaction (R1) is only the first of a series of steps; even if it determines the overall rate it still depends on the concentration of the product, O_2^-, which in turn depends on the rates of the subsequent steps. Therefore, some variation of the overall rate, including a dependence on the surface orientation, is compatible with an outer-sphere mechanism for the first step.

Computational Details

Theory

We have presented our theory for electrocatalytic reactions in various publications.[14,19,23] The new feature that we want to explain herein is the treatment of the solvation for both the initial and the final states. In terms of Marcus theory,[16,24] the pmfs for the approach to the surface are work terms. We denote the energy of solvation of the initial state O_2 by w_i, and of the final state of O_2^- by w_f; both are a function of the distance from the electrode. The corresponding terms in our model Hamiltonian are $n_a w_f + (1-n_a) w_i$, in which n_a n_a is the occupation operator for the orbital under consideration, which in our case is the $1\pi_g$ orbital with spin up and directed towards the surface. Therefore, the terms of our model Hamiltonian pertaining to the reactant and the solvent are given by Equation (1):

$$H_1 = [\varepsilon_a + \Phi - 2\lambda q + w_f - w_i] n_a + w_i + \lambda q^2 \quad (1)$$

in which ε_a is the energy of the orbital a in the vacuum, Φ denotes the effect of the electrode potential, λ is the energy of reorganisation, and q is the solvent coordinate; for a full explanation of the solvent terms, see Refs. [15, 19, 23]. Instead of including the bulk energies of solvation in w_f and w_i, we can just as well use the respective pmfs; this simply amounts to a change of the energy reference and has no effects on the results. The Hamiltonian terms describing the metal and its interaction with the reactant's orbital are given by Equation (2):

$$H_2 = \sum_k \varepsilon_k c_k + \sum_k \left[V_k c_k^+ c_a + V_k^* c_a^+ c_k \right] \quad (2)$$

in which k labels the states of the metal with energies ε_k, and c and c^+ are annihilation and creation operators for the indicated states, respectively.

We first consider the situation far from the electrode, at which the interaction of the reactant with the metal is so small that it has no noticeable effect on the energy—in practice, a separation of 5–6 Å is sufficient. Then the initial state is in equilibrium for $q=0$, and has an energy of w_i. The final state is in equilibrium for $q=1$ and has an energy of $w_f + \varepsilon_a + \Phi - \lambda$. Therefore the reaction is in equilibrium for Equation (3):

$$\Phi_0 = w_i - w_f + \lambda - \varepsilon_a \quad (3)$$

The cathodic overpotential is defined by $-e_0\eta = \Phi - \Phi_0$, so that the free energy of the reaction is $-e_0\eta$; Φ is the electrode potential measured with respect to the Fermi level of the electrode.

The DOS corresponding to the model Hamiltonian $H = H_1 + H_2$ is then given by Equation (4):

$$\rho_a(\varepsilon) = -\frac{1}{\pi} \Im \frac{1}{\varepsilon - [\varepsilon_a + \Phi + w_f - w_i - 2\lambda q + \Lambda(\varepsilon)] + i\Delta(\varepsilon)} \quad (4)$$

in which $\Im$ denotes the imaginary part, and $\Lambda(\varepsilon)$ and $\Delta(\varepsilon)$ are the two chemisorption functions in standard notation.[19,25]

If we delete all the terms pertaining to the solvent, we obtain the corresponding DOS for the molecule in the vacuum [Eq. (5)]:

$$\rho_a(\varepsilon)^{vac} = -\frac{1}{\pi} \Im \frac{1}{\varepsilon - [\varepsilon_a + \Lambda(\varepsilon)] + i\Delta(\varepsilon)} \quad (5)$$

The actual calculations proceeded as before :[14,19,23] We first performed DFT calculation for O_2 at various distances from the Ag(100) surface, obtaining both the energy and the DOS of the molecule. By fitting these results to our model, we determined the interaction parameters of the orbital with the electrode, which are split into the interaction with the d and with the sp bands. These interaction parameters yielded the two chemisorption functions.[25] We then calculated the energy as a function of the distance and compared the results with those obtained from DFT. In our case, the difference between the DFT results and those from our model were less then 0.1 eV, so it was not necessary to correct the results of our model. We then put the solvent and work terms into the DOS, and calculated the energy as a function of the distance and of the solvent parameter q to obtain the surfaces shown in the main part of the article Figures 6–8.

Technical Details of the Molecular Dynamics

To calculate the PMF canonical ensemble (constant NVT), a steered-molecular dynamics simulation was conducted for 1 ns at 298 K on a simulation box containing a Ag(100) slab with three metal layers (thickness 4.09 Å), an ensemble of 470 water molecules, and the O_2 or O_2^- species. Previously an equilibration run of 700 ps was performed. Periodic boundary conditions were set in

the *x* and *y* directions, and the Ewald summation method was used to handle with long range electrostatic interactions.

The well-known 12-6 Lennard–Jones pairwise potential was used to model the interactions between species. For water, we used the SPC/E (extended simple point charge) model and the corresponding parameters for oxygen and hydrogen were taken from Yoshida et al..[26] The Lennard–Jones parameters for silver were taken from Agrawal et al.[27] and for the O_2 and the O_2^- species the parameters were taken from Poling et al.[28] and Shen et al.,[29] respectively. The cross interactions were computed through the Lorentz-Berthelot mixing rules, $\varepsilon_{ij} = \sqrt{\varepsilon_{ii}\varepsilon_{jj}}$, and $\sigma_{ij} = (\sigma_{ii} + \sigma_{jj})/2$.

All simulations were performed by using the LAMMPS (large-scale atomic/molecular massively parallel simulator) code[30] with a time step equal to 2.0 fs. The average temperature of 298 K was maintained by using a Nose-Hoover thermostat with a relaxation time of 0.1 ps.

Technical Details of the DFT Calculations

Periodic DFT calculations were performed by using the DACAPO[31] code with implemented Vanderbilt[32] ultrasoft pseudopotentials for the representation of the atomic cores. A PBE (Perdew, Burke, Ernzerhof)[33] functional and a set of plane waves with a cutoff energy of 350 eV (400 eV for the density) were chosen to describe the valence electrons. Brillouin zone integration[34] was performed using 4 k points in the *x* and *y* directions, and one *k* point in the *z* direction. The surface was represented by 3 layers of silver atoms. and a 3×3 unit cell was employed.

Acknowledgements

Financial support by the Deutsche Forschungsgemeinschaft (FOR 1376) is gratefully acknowledged. E.S. and W.S. thank CONICET for continued support. E.S. acknowledges PIP-CONICET 112-2010001-00411, and PICT- 2012-2324 (Agencia Nacional de Promoción Científica y Tecnológica, FONCYT, préstamo BID) for support. L.M.C.P. thanks the Conselho Nacional de Desenvolvimento Científico e Tecnológico (CNPq/CsF 203178/2014-9) for a fellowship. A generous grant of computing time from the Baden-Württemberg grid is gratefully acknowledged.

Keywords: density functional calculations · electrochemistry · electron transfer · oxygen · silver

[1] X. Ge, A. Sumboja, D. Wuu, T. An, B. Li, F. W. Thomas Goh, T. S. Andy Hor, Y. Zong, Z. Liu, *ACS Catal.* **2015**, *5*, 4643.
[2] R. Adzic in *Electrocatalysis* (Eds.: J. Lipkowski, P. N. Ross), Wiley-VCH, Weinheim, **1998**.
[3] N. Ramaswamy, S. Mukerjee, *Adv. Phys. Chem.* **2012**, DOI: 10.1155/2012/491604, and references therein.
[4] B. B. Blizanac, P. N. Ross, N. M. Markovic, *J. Phys. Chem.* **2006**, *110*, 4735.
[5] N. M. Marcovic, R. R. Adzic, V. B. Vesovic, *J. Electroanal. Chem.* **1984** *163*, 121;N. M. Marcovic, R. R. Adzic, V. B. Vesovic, *J. Electroanal. Chem.* **1983**, *165*, 105.
[6] S. Strbac, R. E. Adzic, *Electrochim. Acta* **1996**, *41*, 2903.
[7] P. Quaino, N. B. Luque, R. Nazmutdinov, E. Santos, W. Schmickler, *Angew. Chem. Int. Ed.* **2012**, *52*, 12997; *Angew. Chem.* **2012**, *124*, 13171.
[8] P. Vassilev, M. Koper, *J. Phys. Chem. C* **2007**, *111*, 2607.
[9] Wei-Xue Li, C. Stanpfl, M. Scheffler, *Phys. Rev. Lett.* **2003**, *90*, 256102.
[10] F. Buatier de Mongeot, M. Rocca, A. Cupolillo, U. Valbusa, H. J. Kreuzer, S. H. Payne, *J. Chem. Phys.* **1997**, *106*, 711.
[11] M. Gajdos, A. Eichler, J. Hafner, *Surf. Sci.* **2003**, *531*, 272.
[12] A. Groß, *Theoretical Surface Science*, Springer, Berlin, **2003**.
[13] L. M. C. Pinto, E. Spohr, P. Quaino, E. Santos, W. Schmickler, *Angew. Chem. Int. Ed.* **2013**, *52*, 7883; *Angew. Chem.* **2013**, *125*, 8037.
[14] E. Santos, P. Quaino, W. Schmickler, *Phys. Chem. Chem. Phys.* **2012**, *14*, 11224.
[15] W. Schmickler, E. Santos *Interfacial Electrochemistry*, 2nd ed., Springer, Berlin, **2010**.
[16] R. A. Marcus, *J. Chem. Phys.* **1956**, *24*, 966.
[17] T. Visart de Bocarmé, T.-D. Chau, F. Tielens, J. Andrés, P. Gaspard, R. L. C. Wang, H. J. Kreuzer, N. Kruse, *J. Chem. Phys.* **2006**, *125*, 054703.
[18] F. Tielens, J. Andrés, T.-D. Chau, T. Visart de Bocarmé, N. Kruse, P. Geerlings, *Chem. Phys. Lett.* **2006**, *421*, 433.
[19] E. Santos, A. Lundin, K. Pötting, P. Quaino, W. Schmickler, *Phys. Rev. B* **2009**, *79*, 235436.
[20] T. Iwasita, W. Schmickler, J. W. Schultze, *Ber. Bunsen-Ges.* **1985**, *89*, 138.
[21] T. Iwasita, W. Schmickler, J. W. Schultze, *J. Electroanal. Chem.* **1985**, *194*, 355.
[22] E. Santos, T, Iwasita, W. Vielstich, *Electrochim. Acta* **1986**, *31*, 431.
[23] E. Santos, W. Schmickler in *Fuel Cell Catalysis: A Surface Science Approach* (Ed.: M. Koper), Wiley, Hoboken, **2009**.
[24] R. A. Marcus, *J. Phys. Chem.* **1963**, *67*, 2889.
[25] S. Davison, K. Sulston, *Green-Function Theory of Chemisorption*, Springer, Dordrecht, **2006**.
[26] K. Yoshida, T. Yamaguchi, A. Kovalenko, F. Hirata, *J. Phys. Chem. B* **2002**, *106*, 5042.
[27] P. M. Agrawal, B. M. Rice, D. L. Thompson, *Surf. Sci.* **2002**, *515*, 21.
[28] B. E. Poling, J. M. Prausnitz, J. P. O'Connell, *Properties of Gases and Liquids*, 5th ed., McGraw-Hill Education, New York, **2001**.
[29] J. Shen, C. F. Wong, J. A. McCammon, *J. Comput. Chem.* **1990**, *11*, 1003.
[30] S. Plimpton, *J. Comput. Phys.* **1995**, *117*, 1.
[31] G. Kresse, J. Hafner, *Phys. Rev. B* **1993**, *47*, 558; S. R. Bahn, K. W. Jacobsen, *Comput. Sci. Eng.* **2002**, *4*, 56.
[32] D. Vanderbilt, *Phys. Rev. B* **1990**, *41*, 7892.
[33] J. P. Perdew, K. Burke, M. Ernzerhof, *Phys. Rev. Lett.* **1996**, *77*, 3865.
[34] D. J. Chadi, M. L. Cohen, *Phys. Rev. B* **1973**, *8*, 5747.

Manuscript received: November 14, 2015
Accepted Article published: December 23, 2015
Final Article published: January 21, 2016